

1 **Impacts of different types of El Niño events on water quality over the** 2 **Corn Belt, United States**

3 Pan Chen^{1,2}, Wenhong Li^{2,*} and Keqi He²

4 ¹ College of Water Resources Science and Engineering, Taiyuan University of Technology, Taiyuan 030024, China

5 ² Earth and Climate Sciences, Nicholas School of the Environment, Duke University, NC 27708, USA

6 *Correspondence to:* Wenhong Li (wenhong.li@duke.edu)

7 **Abstract.** The United States Corn Belt region, which primarily includes two large basins, namely, the Ohio-Tennessee River
8 Basin (OTRB) and the Upper Mississippi River Basin (UMRB), is responsible for the Gulf of Mexico hypoxic zone. Climate
9 patterns such as El Niño can affect the runoff and thus the water quality over the Corn Belt. In this study, the impacts of
10 eastern Pacific (EP) and central Pacific (CP) El Niños on water quality over the Corn Belt region were analyzed using the
11 Soil and Water Assessment Tool (SWAT) models. Our results indicated that at the outlets, annual total nitrogen (TN) and
12 total phosphorus (TP) loads decreased by 13.1% and 14.0% at OTRB, 18.5% and 19.8% at UMRB, respectively, during the
13 EP-El Niño years, whereas during the CP-El Niño years, they increased by 3.3% and 4.6% at OTRB, 5.7% and 4.4% at
14 UMRB, respectively. On the sub-basin scales, more sub-basins showed negative (positive) anomalies of TN and TP during
15 EP- (CP-) El Niño. Seasonal study confirmed that water quality anomalies showed opposite patterns during EP- and CP-El
16 Niño years. At the outlet of OTRB, seasonal anomalies in nutrients matched the El Niño-Southern Oscillation (ENSO)
17 phases, illustrating the importance of climate variables associated with the two types of El Niño on water quality in the
18 region. At the UMRB, TN and TP were also influenced by agriculture activities within the region and their anomalies
19 became greater in the growing seasons during both EP- and CP-El Niño years. Quantitative analysis of precipitation,
20 temperature, and their effects on nutrients suggested that precipitation played a more important role than temperature did in
21 altering water quality in the Corn Belt region during both types of El Niño years. We also found specific watersheds (located
22 in Iowa, Illinois, Minnesota, Wisconsin, and Indiana) that faced the greatest increases in TN and TP loads, were affected by
23 both the precipitation and agricultural activities during the CP-El Niño years. The information generated from this study may
24 help proper decision-making for water environment protection over the Corn Belt.

25

26

27

28

29

30 **1 Introduction**

31 The Corn Belt region of the United States (U.S.) primarily includes the Ohio-Tennessee River Basin (OTRB) and the Upper
32 Mississippi River Basin (UMRB) (Kellner and Niyogi, 2015; Panagopoulos et al., 2017; Ting et al., 2021). The Corn Belt is
33 a very important area of the agricultural activity of the country, as 75% of the corn and 60% of the soybean produced in the
34 U.S. are grown in the region (Thaler et al., 2021). The region's agricultural activities such as fertilizers contribute to the
35 increase of nitrogen and phosphorus levels, which are responsible for the Gulf of Mexico hypoxic zone (Panagopoulos et al.,
36 2014, 2015; Rabalais et al., 2007). The required nutrient reduction of the Corn Belt to decrease hypoxia is the highest among
37 all regions in the Mississippi River Basin (Mississippi River/Gulf of Mexico Watershed Nutrient Task Force, 2011). Hence,
38 water quality changes in the Corn Belt region have been receiving considerable attention.

39 The El Niño-Southern Oscillation (ENSO) is a coupled ocean-atmosphere phenomenon that occurs across the tropical
40 Pacific (Trenberth, 1997; Wang and Kumar, 2015). Precipitation and temperature are influenced by ENSO in many places in
41 the U.S., including the Corn Belt region (Gershunov, 1998; Lee et al., 2014; Thomson et al., 2003; Wang and Asefa, 2018).
42 For example, more frequent dry conditions were found east of the Ohio River in the early spring of a decaying El Niño
43 (Wang and Asefa, 2018). ENSO events could also have a significant impact on the water quality of a basin through changing
44 climate factors. Heavy or prolonged rains might contribute to the pollutant loading from agricultural runoff (Paul et al.,
45 1997). Temperature anomalies might change river water quality by affecting evaporation and water temperature. Keener et al.
46 (2010) showed that ENSO significantly altered water flow and nitrate concentration in a southeastern U.S. basin. Sharma et
47 al. (2012) found that worse water quality in southeast Alabama was linked to the stream temperature anomalies during El
48 Niño years. However, what are the impacts of ENSO on water quality in the Corn Belt region have not been studied.

49 In recent years, studies have found two different types of El Niño events: eastern Pacific (EP) and central Pacific (CP) El
50 Niños (Larkin and Harrison, 2005; Li et al., 2011; Tan et al., 2020; Tang et al., 2016; Yeh et al., 2009). The former has
51 warmer sea surface temperature anomalies (SSTAs) in the Niño 3 region (5°N–5°S, 150°W–90°W), while the latter, also
52 called El Niño Modoki, is manifested by maximum SSTAs in the Niño 4 region (5°N–5°S, 160°E–150°W). The effects of
53 these two types of El Niño on regional climate and runoff are different. For example, reduced rainfall was found in the
54 northern, central, and eastern parts of the Amazon during the EP-El Niño years (EP-ENYs), while increased rainfall
55 anomalies were observed in most of the Amazon during the CP-El Niño years (CP-ENYs) (Li et al., 2011). CP-El Niños
56 were more effective in causing drought conditions in India due to atmospheric subsidence than EP-El Niños (Kumar et al.,
57 2006). How these two types of El Niño affect the water quality of the Corn Belt has not been studied. Over recent years, EP-
58 El Niño has appeared less frequently, whereas CP-El Niño has become more common (Kao and Yu, 2009; Yeh et al., 2009).
59 In the future, CP-El Niño will likely happen more frequently (Yeh et al., 2009; Yu et al., 2010). Understanding the impact of
60 these different El Niño events on water quality over the Corn Belt is of critical importance for the water quality management
61 of streams and rivers.

62 In this study, we used the Soil and Water Assessment Tool (SWAT) model to estimate the water quality changes due to
63 EP- and CP-El Niños over the Corn Belt. The SWAT model is widely used to assess climate change and alternative land
64 use/land management scenarios on runoff and nutrients in a basin (Afonso de Oliveira Serrão et al., 2022; Chaplot et al.,
65 2004; Chen et al., 2021; Johnson et al., 2015; Vaché et al., 2002; Zhang et al., 2020). The detailed objectives of this study
66 were to 1) analyze the impacts of the two types of El Niño on water quality in the Corn Belt region, and 2) identify the main
67 climate factors that affect the change in water quality due to these El Niños. Water quality change associated with future El
68 Niño change was also discussed. Such information is particularly important to enable decision-makers to take timely actions
69 to reduce nutrient loading under climate change.

70 **2 Data and methods**

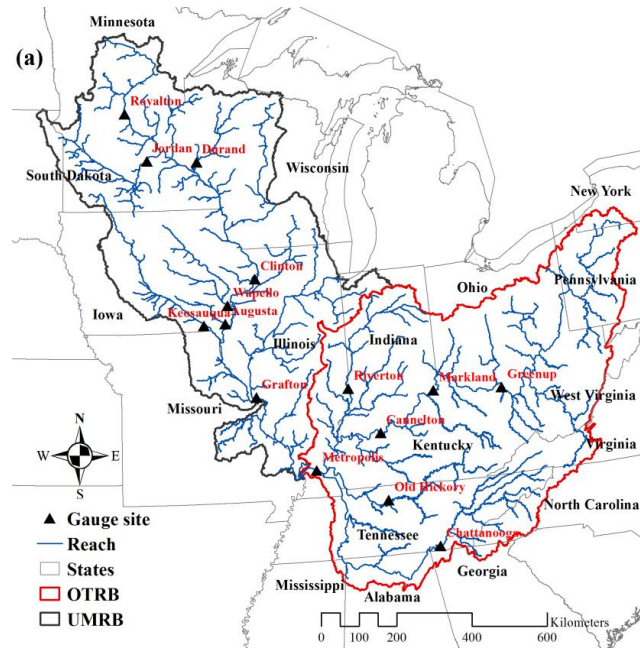
71 **2.1 Data**

72 The study area includes two large basins in the U.S., namely, OTRB (528,000 km²) and UMRB (492,000 km²), as shown in
73 Fig. 1. OTRB comprises a significant portion of Pennsylvania, Ohio, West Virginia, Indiana, Illinois, Kentucky, and
74 Tennessee (Fig. 1a). The amount of annual rainfall in OTRB was high with an average of nearly 1200 mm during 1975–2016.
75 OTRB's slopes are steep, especially in the forested Tennessee basin with slopes greater than 5% in most (60%) of the area.
76 The primary land use types are 50% forest, 20% cropland, and 15% pasture (Fig. 1b). The cropland is mainly grown with
77 corn, soybean, and wheat (Santhi et al., 2006). UMRB mainly includes five states: Iowa, Illinois, Missouri, Wisconsin, and
78 Minnesota (Fig. 1a). The mean annual value of rainfall in UMRB during 1975–2016 was 900 mm. UMRB is relatively flat
79 and most of the basin (75%) has a slope lower than 5%. Cropland is the major land use type of the basin (50%) and is
80 primarily grown with corn and soybean (Fig. 1b).

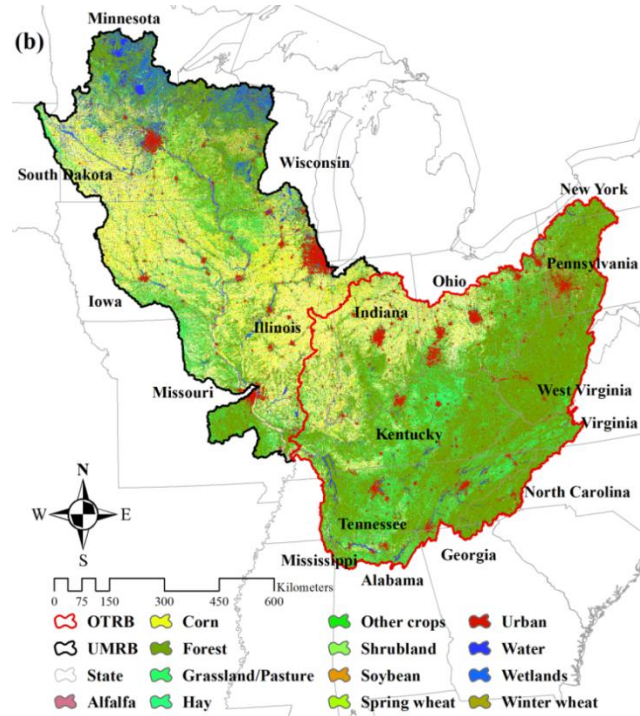
81 The weather data, including precipitation and temperature, were obtained from 2,242 National Weather Service (NWS)
82 stations in the study area. The historical El Niño years were based on Table 1 in Li et al. (2011) and Table 2 in Ren et al.
83 (2018). In summary, nine EP-El Niño events (1976–1977, 1979–1980, 1982–1983, 1986–1987, 1987–1988, 1991–1992,
84 1997–1998, 2006–2007, and 2015–2016) and six CP-El Niño events (1977–1978, 1990–1991, 1994–1995, 2002–2003,
85 2004–2005, and 2009–2010) occurred during the study period (1975–2016).

86 Available monthly streamflow and water quality data from 1975 to 2016 came from the 15 United States Geological
87 Survey (USGS) gaging stations in the study area. The final data used for calibration and validation of the model were shown
88 in Table 1.

89



90



91 **Figure 1.** The Ohio-Tennessee River Basin (OTRB) and Upper Mississippi River Basin (UMRB) (a) available United States
92 Geological Survey (USGS) gage sites (black triangles), reaches (light blue), and the two watersheds (heavy red: OTRB,
93 heavy dark: UMRB) and (b) land use/land cover.

94 **Table 1.** Available periods of measured streamflow, total suspended sediment (TSS), total nitrogen (TN), and total
 95 phosphorus (TP) at 15 USGS gauge at the OTRB and UMRB

Site Name	Site Number	River Basin	Hydrologically Independent	Drainage (km ²)	Streamflow	TSS	TN	TP
Greenup	03216600		Yes	160,579	1975–2019	-	1975–2019	1975–2019
Markland	03277200		No	215,409	1975–2019	-	-	-
Riverton	03342000		Yes	34,087	1975–2019	-	-	-
Old hickory	03426310	OTRB	Yes	30,233	1988–2007	-	-	-
Cannelton	03303280		No	251,229	1975–2019	-	1975–2019	1975–2019
Metropolis	03611500		No	525,768	1975–2014	-	1975–2016	1975–2016
Chattanooga	03568000		Yes	55,426	1975–2008	-	-	-
Royalton	05267000		Yes	30,044	1975–2019	-	-	-
Jordan	05330000		Yes	41,958	1975–2019	-	-	-
Durand	05369500		Yes	23,336	1975–2019	-	-	-
Clinton	05420500		No	221,703	1975–2019	-	1975–2019	1975–2019
Augusta	05474000	UMRB	Yes	11,168	1975–2019	1975–2017	-	-
Wapello	05465500		Yes	32,375	1975–2019	1978–2017	1978–2019	1977–2019
Keosauqua	05490500		Yes	36,358	1975–2019	-	-	-
Grafton	05587450		No	443,665	1975–2019	1989–2017	1989–2019	1989–2019

96

97 Statistical significance of precipitation, temperature, runoff, evaporation, TN, or TP anomalies in El Niño years was tested
 98 by the Monte Carlo method (Mo, 2010). The underlying concept of the method is to use randomness to solve problems that
 99 might be deterministic in principle (Wilks, 1995). Taking TN as an example, in order to test whether TN anomalies in EP-El
 100 Niño years were significantly different from those in normal years, we first composited (i.e., averaged) TN anomalies for the
 101 nine EP-El Niño years. The composite analysis is a useful technique to determine some of the basic structural characteristics
 102 of a climatological phenomenon, such as El Niño which occur over time. We then randomly selected nine years out of 1975-

103 2016 (i.e., keeping the same number of years as the EP-El Niño years) and averaged/composited TN anomalies for the nine
104 randomized years as the first sample. The process was repeated 500 times. These composite samples were used to generate a
105 distribution corresponding to the null hypothesis, against which we could evaluate whether TN anomalies during EP-El Niño
106 were significantly different from those in normal years at a 95% confidence level. Similarly, significance levels of the
107 composite results of precipitation, temperature, runoff, evaporation, and TP anomalies in EP-El Niño years could be
108 determined. Such a method has been widely used in climate-related studies (Laken and Čalogović, 2013; Mo, 2010; Sanchez
109 and Karnauskas, 2021) due to its robustness.

110 **2.2 SWAT model**

111 **2.2.1 Model description**

112 SWAT was developed by the U.S. Department of Agriculture Agricultural Research Services (Arnold et al., 1998). It has
113 been widely used in assessing the effects of climate and land use change on hydrological processes, sediment, and nutrients
114 in a basin (Neitsch et al., 2011; Pagliero et al., 2014; Yen et al., 2016). In the SWAT model, a basin is partitioned into sub-
115 basins, which are further divided into hydrological response units (HRUs) (Gassman et al., 2007; Neitsch et al., 2011;
116 Williams et al., 2008). Runoff, sediment, and nutrient loads are simulated for each HRU and then aggregated for the sub-
117 basins (Chen et al., 2021; Gassman et al., 2007; Neitsch et al., 2011). Thus, the spatial resolution of the model is measured
118 by the number of HRUs and sub-basins. The pollution situation of each sub-basin during different El Niño years could be
119 obtained from this model. The model was calculated on a daily time scale, and the results were analyzed on a monthly time
120 scale.

121 **2.2.2 Model set-up and calibration**

122 In this study, 8-digit Hydrologic Unit Codes (HUC-8) defined by the USGS were selected as SWAT sub-basins. In total, the
123 OTRB and UMRB included 152 and 131 sub-basins, respectively. Flow paths between the sub-basins were determined using
124 the stream network of the National Hydrography Dataset Plus (NHDPlus) dataset developed by the USGS and U.S.
125 Environmental Protection Agency. Each of the sub-basins was further divided into several spatially uniform HRUs based on
126 land use, soil type, and slope (Chen et al., 2021; Neitsch et al., 2011). Thresholds of 0%, 10%, and 5% were used for land
127 use, soil, and slope, respectively, resulting in a total of 20,157 and 20,581 HRUs in the OTRB and UMRB. Then, point
128 sources (Schwarz et al., 2006), crop management (U.S. Department of Agriculture (USDA) - National Agricultural Statistics
129 Service (NASS), 2017), and tillage (Baker, 2011) dataset were incorporated to build the SWAT model (Chen et al., 2021).

130 SWAT Calibration and Uncertainty Programs (SWAT-CUP) with Sequential Uncertainty Fitting (SUFI-2) algorithm was
131 selected in this large-scale study to complete the calibration of the SWAT model (Abbaspour et al., 2012). The parameters of
132 water flow and water quality in OTRB and UMRB were selected based on a manual experimentation with SWAT parameters
133 and a literature review (Chen et al., 2021; Panagopoulos et al., 2014, 2015; Yen et al., 2016). The calibration steps followed

134 a recent study by Chen et al. (2021). The final parameters were shown in Table S1 and S2 in the supplementary materials.
135 The calibration results indicated that the SWAT model could rationally capture the observation (see Section 2.2.3).

136 **2.2.3 Model performance**

137 Overall, SWAT simulated the water flow of the OTRB and UMRB reasonably well in both calibration (1997–2016) and
138 validation (1975–1996) periods (Table 2). The coefficient of determination (R^2) and Nash-Sutcliffe efficiency (NSE) values
139 were larger than 0.5 for almost all the USGS gages except Chattanooga, and percent bias ($PBIAS$) values were all acceptable
140 during the calibration periods (1997–2016) based on the $\leq \pm 25\%$ deviation criterion (Moriassi et al., 2015). The validation
141 results also showed acceptable static values and in some cases were even better, such as Chattanooga and Grafton. Figures
142 S1 and S2 in the supplementary materials further demonstrated good agreement between the calculated and observed
143 streamflow across OTRB and UMRB; particularly, most of the peaks and recession limbs were well matched in the
144 simulations.

145 Modeled water quality was generally in agreement with the observations for the two river basins, as most of the $PBIAS$
146 values were within bias criteria for sediment, TN, and TP during both the calibration and validation periods (Santhi et al.,
147 2014) (Table 3). The only exception that did not meet the criteria was the sediment simulation at Augusta. The upstream
148 drainage area of Augusta was relatively small (only around 3% of the UMRB), thus its influence on downstream sediment
149 and pollutant transport downstream was minor (Fig. 1a). The sediment statistics in OTRB were not calculated here because
150 of a lack of observations (Panagopoulos et al., 2015). Instead, we compared the simulated annual sediment at Metropolis
151 with observations during 1975–2010 and found that the difference was also within the bias criteria for sediment
152 (Panagopoulos et al., 2015; Santhi et al., 2014). Moreover, most of the NSE and R^2 values were positive and many R^2 values
153 were greater than 0.5, indicating that the simulated water quality was reasonable (Chen et al., 2021). This finding could be
154 further proved by the graphs of observed and simulated sediment and nutrients (Figs. S3 and S4).

155
156
157
158
159
160
161
162
163
164
165
166

Table 2. Monthly streamflow calibration and validation statistics.

Gauge Site	Calibration (1997–2016)			Validation (1975–1996)		
	R^2	NSE	$PBIAS$	R^2	NSE	$PBIAS$
Greenup	0.88	0.87	1.6	0.87	0.82	15.9
Markland	0.88	0.87	6.4	0.88	0.81	17.4
Riverton	0.84	0.83	-1.4	0.8	0.78	-7.4
Old Hickory	0.82	0.75	-4.7	0.81	0.79	7.8
Cannelton	0.89	0.87	9.6	0.9	0.84	15.9
Metropolis	0.84	0.83	4.1	0.88	0.8	15.8
Chattanooga	0.59	0.48	6.1	0.62	0.53	10.7
Royalton	0.63	0.56	-4.7	0.58	0.55	-0.5
Jordan	0.64	0.59	0.7	0.77	0.66	-22.8
Durand	0.65	0.5	-20.9	0.6	0.53	-10.7
Clinton	0.63	0.56	6.6	0.63	0.59	9.8
Augusta	0.75	0.7	-9.9	0.78	0.76	-9.9
Wapello	0.71	0.67	-2.3	0.76	0.76	-1
Keosauqua	0.76	0.73	5.8	0.8	0.78	14
Grafton	0.69	0.62	12.5	0.77	0.7	16.1

168

169

Table 3. Monthly TSS, TN, and TP calibration and validation statistics.

Variable	Gauge Site	Calibration(1997–2016)			Validation(1975–1996)		
		R^2	NSE	$PBIAS$	R^2	NSE	$PBIAS$
TSS	Augusta	0.34	0.1	64.5	0.39	0.02	77.2
	Wapello	0.45	0.15	-21.5	0.51	0.48	13.6
	Grafton	0.43	0.22	0.7	0.26	0.07	13.9
TN	Greenup	0.57	0.23	-13.7	0.59	0.52	17
	Cannelton	0.63	0.59	8.3	0.59	0.46	26.9
	Metropolis	0.58	0.36	-9.2	0.57	0.51	14.9
	Clinton	0.43	-0.61	2.7	0.36	-0.25	9.4
	Wapello	0.51	0.05	1.8	0.44	0.32	17.6
	Grafton	0.54	0.15	2.2	0.53	0.08	2
TP	Greenup	0.56	0.46	-29.6	0.59	0.57	8.6
	Cannelton	0.56	0.48	21.2	0.44	0.35	28.1
	Metropolis	0.49	0.41	-8.6	0.45	0.38	-5.2
	Clinton	0.44	-0.59	-11.1	0.42	0.13	10.9
	Wapello	0.6	0.24	-19.1	0.55	0.29	-16.3
	Grafton	0.57	0.25	0.8	0.54	0.12	-14.8

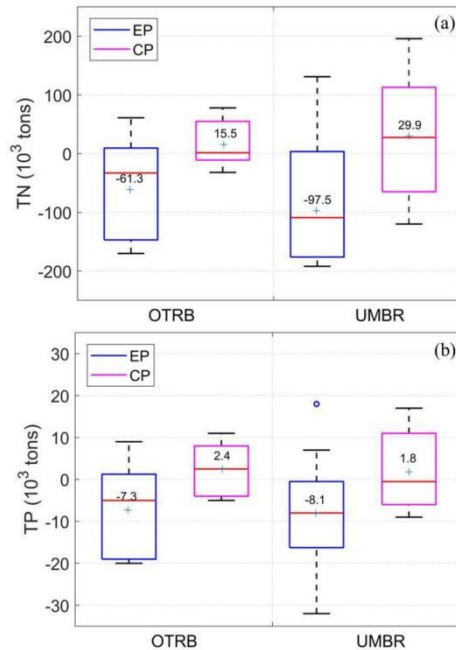
170 **3 Results**

171 **3.1 Impacts of the EP- and CP-El Niños on the water quality in the Corn Belt**

172 **3.1.1 Annual composite**

173 (1) Water quality at the outlet

174 Figure 2 showed the nutrient change during EP- and CP-ENYs at the outlet of OTRB and UMRB. Annual loads of TN and
175 TP decreased during the EP-ENYs, while the pattern reversed during the CP-ENYs in the U.S. Corn Belt region. Specifically,
176 compared to normal years, the TN and TP decreased by 13.1% (61,300 metric ton yr⁻¹, hereafter ton yr⁻¹) and 14.0% (7,300
177 ton yr⁻¹) during EP-ENYs, respectively, whereas they increased by 3.3% (15,500 ton yr⁻¹) and 4.6% (2,400 ton yr⁻¹) during
178 CP-ENYs at the outlet of the OTRB, respectively (Fig. 2). TN and TP at the outlet of the UMRB showed a similar pattern as
179 that of the OTRB, decreasing (increasing) by 18.5% (5.7%) and 19.8% (4.4%) in EP (CP)-ENYs. Furthermore, EP-El Niños
180 had a much greater impact on water quality than CP-El Niños at the outlets of OTRB and UMRB. The magnitudes of
181 variation in both TN and TP during the EP-ENYs were three to four times greater than those during the CP-ENYs (Fig. 2).



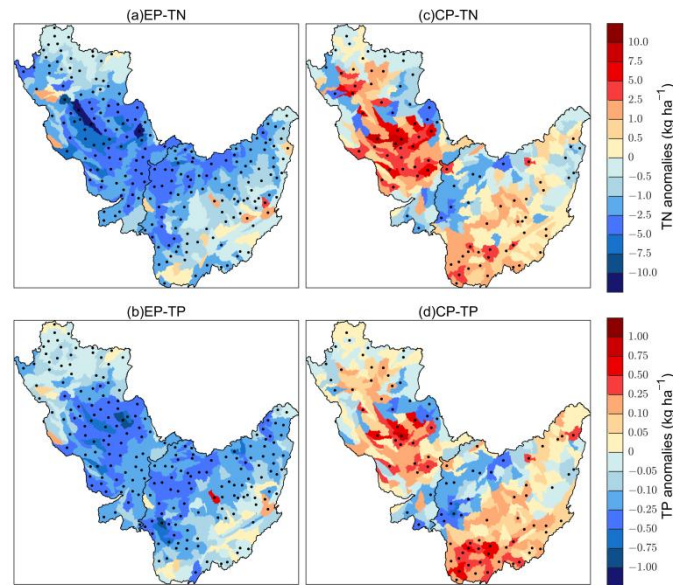
182

183 **Figure 2.** Box plots of annual (a) TN and (b) TP anomalies (unit: 10³ tons) at the outlets of the OTRB and UMRB
184 during EP-El Niño years and CP-El Niño years, respectively. The green plus (+), red solid horizontal line, box, and
185 whisker ends indicate the mean, median, 25th and 75th percentile, and the 10th and 90th percentile, respectively. The data
186 points outside the ranges are shown in hollow dots.

187 (2) Water quality at the sub-basin scale

188 We analyzed water quality change on the sub-basin scale during EP-ENYs and CP-ENYs, respectively (Fig. 3). Anomalous
189 patterns of water quality associated with El Niño events within the Corn Belt varied in space. Clearly, more sub-basins
190 showed negative anomalies of TN and TP during EP-ENYs, whereas more sub-basins showed positive anomalies during CP-
191 ENYs (Fig. 3). Specifically, during EP-ENYs, significant below-average TN and TP were found almost in the whole OTRB
192 and UMRB with maximum reductions of TN and TP up to -11.7 and -0.9 kg ha^{-1} , respectively, which were of similar
193 magnitudes to the mean values (12.7 kg of N ha^{-1} and 1.0 kg of P ha^{-1}) in the Corn Belt region (Figs. 3a and 3b). During CP-
194 ENYs, positive anomalies mainly occurred throughout the southern OTRB and UMRB. In the northern UMRB and OTRB,
195 about 42.4% and 41.7% of sub-basins tended to have below-average TN and TP (Figs. 3c and 3d). These patterns coincided
196 with the TN and TP changes at the outlets of the two basins, which could also explain why greater changes in TN and TP
197 occurred in EP-ENYs than in CP-ENYs at the outlets of the OTRB and UMRB (Fig. 2).

198



199

200 **Figure 3.** Composite results of annual TN and TP anomalies (unit: kg ha^{-1}) in EP-El Niño years (a and b) and in CP-El Niño
201 years (c and d) during the period of 1975–2016. Stippling denotes anomalies significantly different from zero at the 95%
202 confidence level based on the Monte Carlo test.

203 3.1.2 Seasonal composite

204 (1) Water quality at the outlet

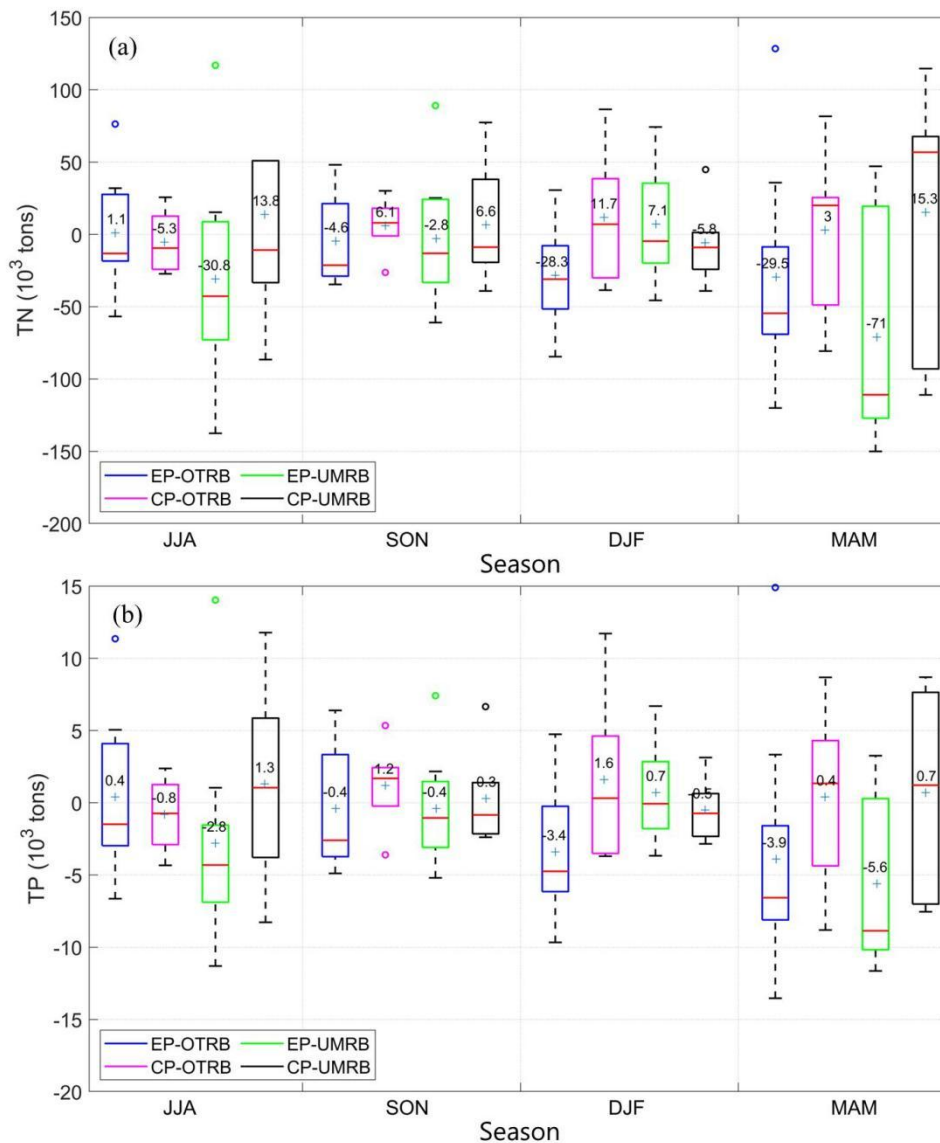
205 Figure 4a showed TN anomalies at the OTRB and UMRB outlets in each season during EP- and CP-ENYs. At the outlet of
206 the OTRB, seasonal anomalies of the water quality reached the maximum when ENSO signals were the strongest (Fig. 4a).

207 El Niño usually developed in boreal summer (June-August, JJA) and autumn (September-November, SON), peaked in
208 winter (December of the current year and January and February of the following year, DJF), and decayed in spring (March-
209 May, MAM) (Trenberth, 1997; Li et al., 2011). Maximum changes in TN occurred in the winter and spring seasons during
210 EP-ENYs (decreased by 28.3×10^3 and 29.5×10^3 metric tons (hereafter ton), respectively, Fig. 4a). During CP-ENYs, TN
211 increased by 11.7×10^3 tons in winter, and did not change much in the rest of the three seasons (spring, summer, and autumn)
212 compared to that in the normal years (Fig. 4a). Seasonal TN anomalies at the outlet of the UMRB were different from those
213 of the OTRB. Figure 4a showed that TN decreased by 71.0×10^3 and 30.8×10^3 tons, respectively, in the spring and summer
214 seasons during EP-ENYs; but in winter and autumn, TN did not change much compared to normal years. Similarly, during
215 CP-ENYs, TN anomalies were greater in spring and summer although TN anomalies became positive during CP-ENYs,
216 different from TN changes during EP-ENYs (Fig. 4a).

217 Figure 4b demonstrated that the seasonal changes of TP during EP- and CP-ENYs were similar to those of TN in both
218 OTRB and UMRB during EP-ENYs. At the OTRB the magnitudes of TP reduction in boreal winter and spring were greater
219 than those in the summer and autumn seasons during EP-ENYs. During CP-ENYs, TP anomalies were greater in both
220 autumn and winter (Fig. 4b). This phenomenon was probably related to the different duration of the two types of El Niño.
221 The mean duration of EP-El Niño was about 15 months (Mo, 2010), its impact on water quality could last into the following
222 spring; while El Niño Modoki usually lasted for about eight months (Mo, 2010, Yu et al., 2010), therefore the impacts of the
223 CP-El Niño on water quality usually ended in the winter. Besides, at the UMRB maximum changes in TP occurred in the
224 spring and summer seasons during both EP- and CP-ENYs.

225 In summary, more seasons showed negative anomalies of water quality during EP-ENYs, whereas more seasons showed
226 positive anomalies during CP-ENYs (Fig. 4). Consequently, the annual TN and TP anomalies over the Corn Belt region
227 showed the opposite pattern during EP-ENYs and CP-ENYs (Fig.2).

228



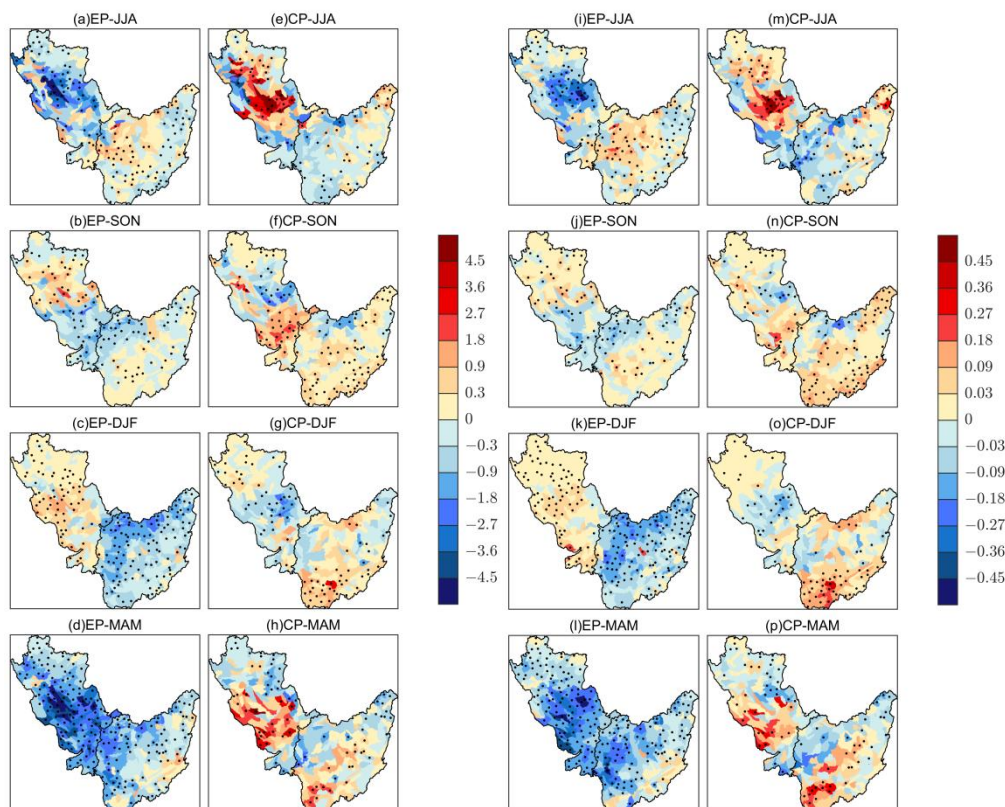
229

230 **Figure 4.** Same as Fig. 2 but for seasonal scales, i.e., summer (June-August, JJA), autumn (September-November,
 231 SON), winter (December of the current year and January and February of the following year, DJF), and spring (March-
 232 May, MAM).

233 (2) Water quality at the sub-basin scale

234 Water quality at the Corn Belt can vary in different locations/sub-basins and change between seasons. Figure 5 showed
 235 spatial patterns of TN and TP anomalies at the OTRB and UMRB in each season during the CP- and EP-ENYs, separately.
 236 EP-El Niño was characterized by negative TN and TP anomalies over most of the OTRB and UMRB for all seasons (Figs.

237 5a–5d and 5i–5l). Significant below-average TN and TP occurred in almost all of the UMRB and the eastern OTRB in the
 238 summer when EP-El Niño was developing in the tropical Pacific, with maximum reductions up to -4.5 and -0.45 kg ha^{-1} ,
 239 respectively (Figs. 5a and 5i). The negative water quality anomalies moved to the southern UMRB and northern OTRB in
 240 the autumn (Figs. 5b and 5j). These negative anomalies further moved to the whole OTRB when EP-El Niño was mature in
 241 the winter (Figs. 5c and 5k). This result generally agreed with previous findings of the El Niño impacts on the precipitation
 242 in the study area, which indicated that the precipitation in the Ohio Valley was sensitive to El Niño events and showed
 243 negative precipitation anomalies at EP-ENYs (Mo, 2010; Twine et al., 2005). In spring, severe TN and TP deficits were most
 244 apparent almost all over the Corn Belt area (Figs. 5d and 5l).



245
 246 **Figure 5.** Seasonal composite of (a-h) TN and (i-p) TP anomalies (unit: kg ha^{-1}) in summer (JJA) (a and i), autumn (SON) (b
 247 and j), winter (DJF) (c and k), and spring (MAM) (d and l) in EP-El Niño years during the period of 1975–2016; (e-h) and
 248 (m-p) are the same as (a-d) and (i-l) but for CP-El Niño years. Stippling denotes anomalies significantly different from zero
 249 at the 95% confidence level based on the Monte Carlo test.

250 In contrast, during CP-ENYs, positive TN and TP anomalies were scattered in most of the Corn Belt region with the
 251 highest TN and TP anomalies increase up to 4.5 and 0.45 kg ha^{-1} , respectively (Figs. 5e–5h and 5m–5p). In summer,
 252 northern UMRB and eastern OTRB were characterized by above-normal water quality (Figs. 5e and 5m). The positive TN
 253 and TP anomalies moved to the southern UMRB and whole OTRB in the autumn (Figs. 5f and 5n). In winter, these positive

254 anomalies were concentrated in the southern OTRB and northern UMRB (Figs. 5g and 5o). In the spring, abnormally high
255 TN and TP mainly occurred in the southern part of the UMRB while most of the positive and negative anomalies in the
256 OTRB region were insignificant (Figs. 5h and 5p).

257 In conclusion, water quality anomalies showed opposite patterns during EP-ENYs and CP-ENYs on both annual and
258 seasonal time scales in the Corn Belt region. Furthermore, EP-El Niño seemed to have a greater and long-lasting impact on
259 TN and TP than CP-El Niño. Hence, treating the two as a single phenomenon was not appropriate when analyzing the
260 impacts of ENSO on water quality.

261 **3.2 Possible climate reasons for the water quality change during CP- and EP-El Niño events**

262 As precipitation and temperature usually respond differently to the two types of El Niño at different temporal and spatial
263 scales (Li et al., 2011; Tan et al., 2020), we hereafter analyzed these climate factors' impacts accordingly in the Corn Belt
264 region.

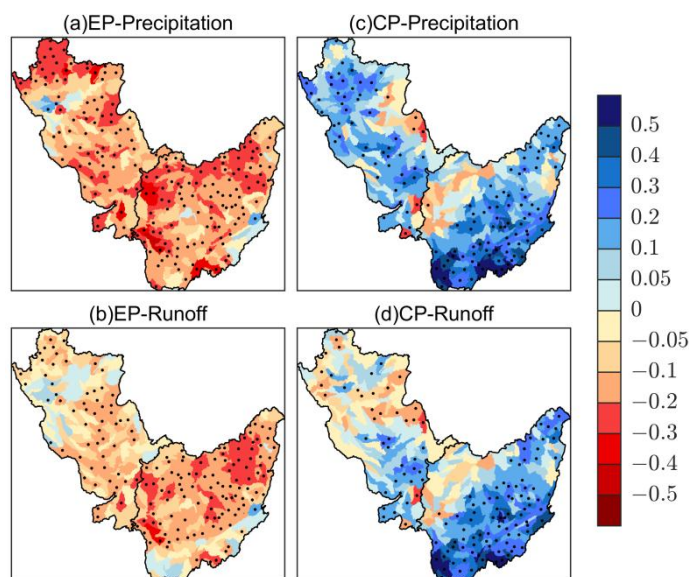
265 **3.2.1 Precipitation**

266 Decreased precipitation in EP-ENYs was one of the important reasons that improved water quality in the Corn Belt region.
267 This finding could be shown in the spatial patterns of annual precipitation (Fig. 6a), and TN and TP anomalies (Figs. 3a and
268 3b). For example, significantly below-normal precipitation occurred in much of the OTRB and UMRB (278 out of 283 sub-
269 basins) during EP-ENYs (Fig. 6a), thus TN and TP were reduced in most parts of the Corn Belt (Figs. 3a and 3b). During
270 CP-ENYs, precipitation anomalies became positive in 226 out of 283 sub-basins (Fig. 6c). Correspondingly, TN and TP
271 concentrations were elevated compared to normal years (Figs. 3c and 3d). Spatially, there were more sub-basins (98.2%) and
272 larger area with negative precipitation anomalies in EP-ENYs than positive anomalies (79.9% sub-basins) during CP-ENYs
273 in the Corn Belt, indicating that EP-El Niño tended to have a much wider impact on precipitation and thus water quality than
274 CP-El Niño.

275 To better understand how precipitation affected water quality in the Corn Belt, variations of annual runoff during EP-
276 ENYs and CP-ENYs were also discussed because nitrogen and phosphorus were transported by runoff (Neitsch et al., 2011),
277 and precipitation was a very important source of runoff (Gassman et al., 2007). The overall patterns of runoff anomalies
278 (Figs. 6b and 6d) were similar to those of precipitation anomalies (Figs. 6a and 6c) during the two types of El Niño with
279 pattern correlations being 0.79 at OTRB and 0.75 at UMRB in EP-ENYs, 0.96 and 0.77 in CP-ENYs, respectively.
280 Specifically, during EP-ENYs, negative annual runoff anomalies occurred in most of the Corn Belt region (Fig. 6b),
281 resulting in reduced TN and TP compared to normal years (Figs. 3a and 3b). In contrast, in CP-ENYs, positive runoff
282 anomalies were mainly concentrated in southern OTRB and UMRB (Fig. 6d), more nutrients were thus carried out by the
283 runoff associated with above-normal precipitation in the area (Figs. 3c and 3d). We also noticed that EP-El Niño had a wider
284 influence on runoff than CP-El Niño, as 71 more sub-basins (259 vs 188) and larger areas with significant runoff anomalies
285 were found in EP-ENYs than in CP-ENYs (Figs. 6b and 6d), generally consistent with the spatial patterns of precipitation

286 changes due to the El Niños (Figs. 6a and 6c). The phenomena could partly explain why EP-El Niños tended to have greater
287 impacts on the water quality than CP-El Niños at the outlets of the OTRB and UMRB.

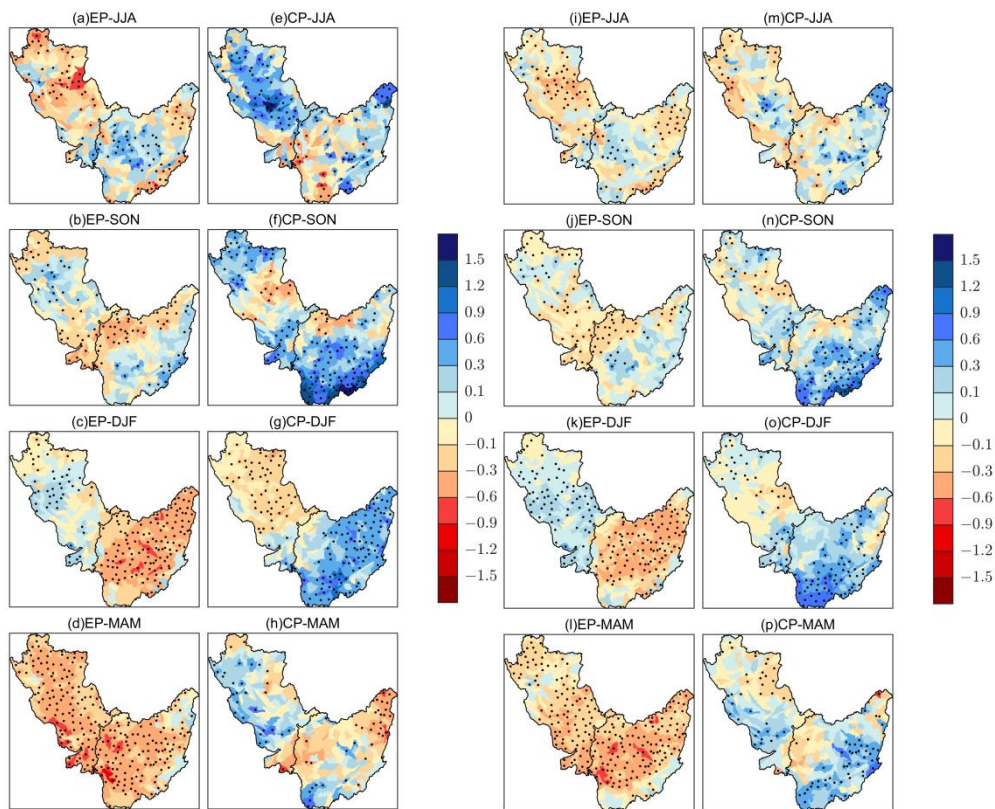
288 Some differences also existed among precipitation, runoff, and nutrients. For precipitation and runoff, annual precipitation
289 anomalies were greater than runoff anomalies in the El Niño years. For example, precipitation anomalies of many sub-basins
290 in northern UMRB were stronger than -0.2 mm day^{-1} during EP-ENYs, but the magnitudes of runoff anomalies were
291 weaker than -0.2 mm day^{-1} (Figs. 6a and 6b). During CP-ENYs, most annual precipitation and runoff anomalies were
292 positive, but the magnitudes of precipitation anomalies were generally higher than that of runoff anomalies (Figs. 6c and 6d).
293 These findings suggested that the impact of El Niño on runoff was weakened by the land surface hydrological process. For
294 runoff and nutrients, changes of runoff in El Niño years were greater in the OTRB than in the UMRB (Figs. 6b and 6d),
295 whereas changes of TN and TP were smaller in the OTRB than in the UMRB during both EP-ENYs and CP-ENYs (Fig. 3).
296 The discrepancies between annual runoff and nutrient anomalies in the OTRB and UMRB may be related to the presence of
297 more cropland in the UMRB where more fertilizers were used (Chen et al., 2021, see Section 4.1 for details), hence a
298 relatively small change of runoff due to El Niño-induced precipitation could lead to large TN and TP variations.



299
300 **Figure 6.** Composite of annual precipitation and runoff anomalies (unit: mm day^{-1}) for the two types of El Niño during the
301 period of 1975–2016 (a and b) in EP-El Niño years and (c and d) in CP-El Niño years. Stippling denotes anomalies
302 significantly different from zero at the 95% confidence level based on the Monte Carlo test.

303 Seasonal patterns of precipitation and runoff anomalies (Fig. 7) further proved the impacts of precipitation on water
304 quality through runoff during EP-ENYs and CP-ENYs. In summer, significantly below-normal precipitation occurred in
305 almost all of the UMRB when EP-El Niño was developing in the tropical Pacific, with maximum reductions of precipitation
306 up to -0.9 mm day^{-1} in the region (Fig. 7a). The runoff anomaly pattern was much the same as that of precipitation, but in a

307 weaker magnitude—less than -0.6 mm day^{-1} in UMRB (Fig. 7i). At the same time, TN and TP decreased in the area (Figs.
 308 5a and 5i) because fewer nutrients were carried out by the reduced runoff in summer (Fig. 7i). Similar change patterns of
 309 precipitation (Figs. 7b-7d), runoff (Figs. 7j-7l), and nutrients (Figs. 5b-5d and 5j-5l) could also be found in other seasons
 310 during EP-ENYs. We noticed that negative runoff and precipitation anomalies reached their maximum in spring throughout
 311 the Corn Belt, leading to better water quality in the region compared to the normal years. CP-El Niño events caused the
 312 opposite patterns of seasonal precipitation (Figs. 7e-7h) and runoff anomalies (Figs. 7m-7p) in the Corn Belt region; TN and
 313 TP thus increased in central and southern UMRB in the spring, summer, and autumn, and most of OTRB from autumn to
 314 winter (Figs. 5e-5h and 5m-5p). Some differences also existed between precipitation and water quality in the UMRB,
 315 especially in spring and summer. During these two seasons, the variation of the seasonal precipitation at each sub-basin was
 316 relatively uniform in both EP-ENYs (Figs. 7a and 7d) and CP-ENYs (Figs. 7e and 7h), but nutrient variations were high in
 317 some sub-basins of the UMRB (Figs. 5a, 5d, 5e, 5h, 5i, 5l, 5m, and 5p). This phenomenon suggested that water quality was
 318 also influenced by local factors besides climate variables associated with El Niños.



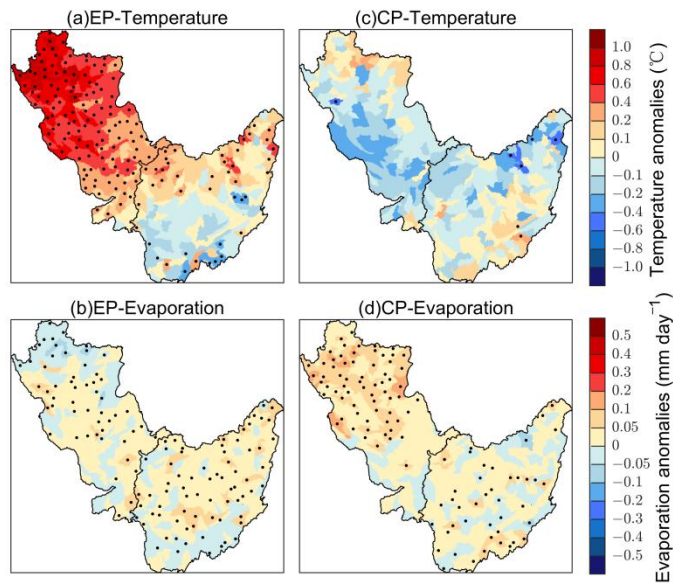
319
 320 **Figure 7.** Composite of seasonal (a-h) precipitation and (i-p) runoff anomalies (unit: mm day^{-1}) in JJA (a and i), SON (b and
 321 j), DJF (c and k), and MAM (d and l) in EP-El Niño years during the period of 1975–2016; (e-h) and (m-p) are the same as
 322 (a-d) and (i-l) but for CP-El Niño years. Stippling denotes anomalies significantly different from zero at the 95% confidence
 323 level based on the Monte Carlo test.

324 3.2.2 Temperature

325 Temperature changes have previously been found to affect water quality by changing the evaporation process of the water
326 cycle (Neitsch et al., 2011 Sun et al., 2011). Thus, how evaporation varied associated with temperature change during El
327 Niños in the Corn-Belt region was analyzed. Compared to normal years, the annual temperature increased over the UMRB,
328 but decreased in the OTRB, especially in the southern OTRB during EP-ENYs (Fig. 8a). Evaporation slightly increased in
329 most of OTRB (Fig. 8b), which did not share the same pattern with temperature change on the annual time scale (Fig. 8a).
330 This might be due to the fact that temperature directly affected potential evapotranspiration (Neitsch et al., 2011), the ability
331 of the atmosphere to remove water from the surface through both evaporation and transpiration, but the actual
332 evaporation/evapotranspiration was also related to other variables such as the amount of water available for evaporation
333 besides temperature. Enhanced evaporation further reduced runoff (Bales et al., 2017). Thus, decreased precipitation (Fig. 6a)
334 and enhanced evaporation (Fig. 8b) during the EP-ENYs would facilitate runoff decline and cause a much wider impact of
335 EP-El Niño events on water quality in the Corn Belt region (Fig. 3). During CP-ENYs, temperature decreased insignificantly
336 in most of the Corn Belt region (Fig. 8c). Evaporation increased in more sub-basins over the UMRB (Fig. 7d). The enhanced
337 evaporation (Fig. 8d) tended to offset, to some extent, the impact of higher than normal precipitation (Fig. 6c) on water
338 quality during CP-ENYs.

339 The impacts of the two climate factors, precipitation and temperature (through evaporation), on runoff were compared.
340 During the El Niño years, the magnitude of annual precipitation change was often greater than 0.1 mm day^{-1} (Figs. 6a and 6c)
341 while most of the annual evaporation varied between -0.05 and 0.05 mm day^{-1} (Figs. 8b and 8d). This suggested that both
342 precipitation and evaporation influence water quality through runoff, but precipitation seemed to play a more important role
343 in altering water quality over the Corn Belt region during El Niño years.

344

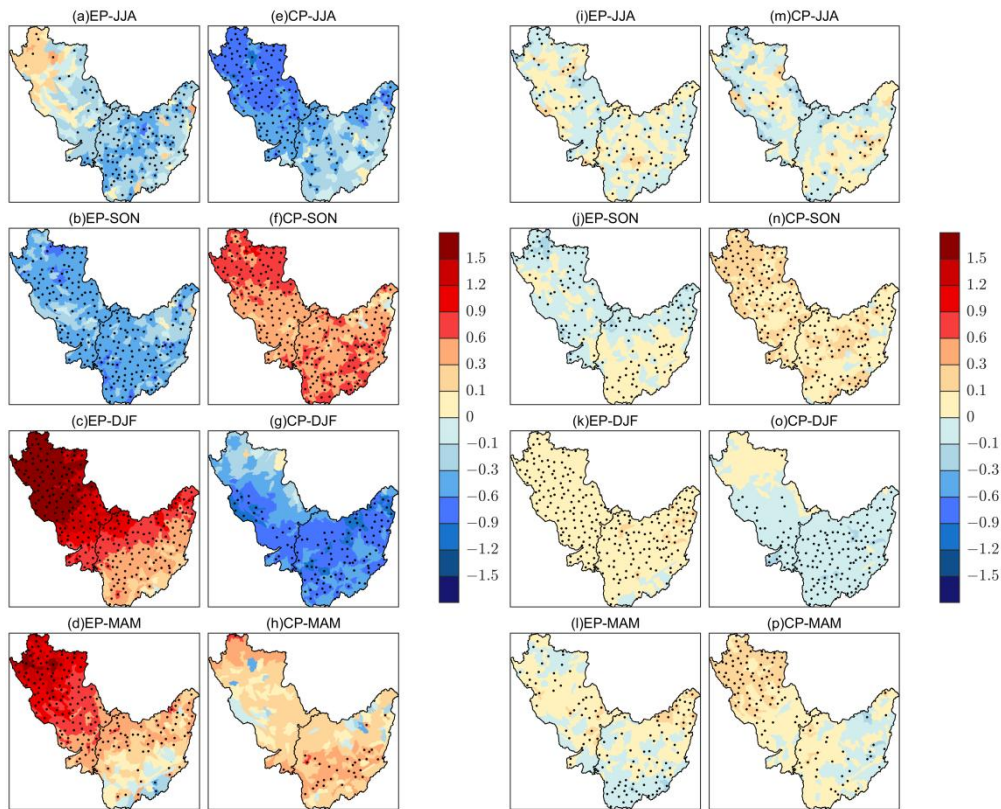


345

346 **Figure 8.** Composite results of annual average temperature (a and c, unit: °C) and evaporation (b and d, unit: mm day⁻¹)
 347 anomalies for EP-El Niño years (a and b) and CP-El Niño years (c and d), respectively. Stippling denotes anomalies
 348 significantly different from zero at the 95% confidence level based on the Monte Carlo test.

349

350 Figure 9 showed seasonal patterns of temperature and evaporation anomalies during the CP- and EP-ENYs. In EP-ENYs,
 351 significantly below-normal temperature occurred throughout the OTRB in the summer (Fig. 9a) and expanded to the entire
 352 Corn Belt region in the autumn (Fig. 9b). In winter and spring, significantly positive temperature anomalies were shown in
 353 the UMRB and most of OTRB (Figs. 9c and 9d). Corresponding to the seasonal temperature anomalies, evaporation varied
 354 differently at different seasons (Figs. 9i-9l). In the summer and autumn, most sub-basins had negative evaporation anomalies
 355 with decreased temperature (Figs. 9i and 9j); but in winter and spring, significantly above-normal evaporation occurred with
 356 increased temperature in EP-ENYs (Figs. 9k and 9l). During CP-ENYs, the summer season was characterized by negative
 357 temperature anomalies throughout the Corn Belt region, with the maximum anomalies up to -1.2 °C (Fig. 9e). Evaporation
 358 anomalies became negative in most sub-basins (Fig. 9m). The temperature pattern was reversed in the autumn, with positive
 359 temperature and evaporation anomalies over the entire region (Figs. 9f and 9n). In winter, temperature anomalies became
 360 negative again (Fig. 9g), evaporation also reduced, with significantly negative anomalies in the OTRB and central and
 361 southern UMRB (Fig. 9o). Temperature anomalies in spring were insignificant (Fig. 9h) most likely due to the short eight-
 362 month duration of the CP-El Niño (Mo, 2010, Yu et al., 2010), although positive evaporation anomalies appeared in the
 363 northern UMRB (Fig. 9p).



364

365 **Figure 9.** Composite results of seasonal temperature (a-h, unit: °C) and evaporation (i-p, unit: mm day⁻¹) anomalies in JJA (a
 366 and i), SON (b and j), DJF (c and k), and MAM (d and l) in EP-El Niño years (a-d, i-l) and CP-El Niño years (e-h, m-p),
 367 respectively. Stippling denotes anomalies significantly different from zero at the 95% confidence level based on the Monte
 368 Carlo test.

369 4 Discussion

370 4.1 Agricultural activity

371 This study focused on climate impact on water quality during EP-ENY and CP-ENY, we did not perform sensitivity
 372 experiments on agriculture activities. In the SWAT model runs, the distribution of agriculture activities pattern (2008
 373 Cropland Data Layers (CDL); USDA-NASS, 2016) was kept the same during El Niño and normal years. Corresponding to
 374 the described agriculture activities, the corn growing areas, i.e., the southern UMRB and northern OTRB, usually produced
 375 greater annual TN loads (>10 kg of N ha⁻¹) and TP loads (>1 kg of P ha⁻¹) (Fig. S5). During EP-ENYs, the nutrients were
 376 largely reduced (>1 kg of N ha⁻¹ and >0.1 kg of P ha⁻¹) in the two corn-growing regions because of decreased precipitation
 377 (< -0.1 mm day⁻¹) (Figs. 3a, 3b, and 6a). In CP-ENYs, the nutrient level increased in the southern UMRB (Figs. 3c and 3d)
 378 since enhanced precipitation in CP-ENYs exacerbated the water quality in the area of heavy agriculture activities (Fig. 6c).

379 Water quality in the OTRB region showed different change patterns from the agriculture activities, i.e., TN and TP decreased
380 in the northern OTRB but increased in the southern OTRB (Figs. 3c and 3d). Such changes in water quality followed the
381 precipitation change in the OTRB (Fig. 6c), demonstrating that CP-El Niño-induced precipitation change played a more
382 important role in modulating water quality in OTRB.

383 On seasonal scales, changes in nutrients' magnitudes were stronger in spring and summer, especially in UMRB (Fig. 5).
384 The heavy loading of nutrients was related to the agriculture activities during the growth period of crops in the Corn Belt.
385 The major crops here are corn and soybean, which are often planted and fertilized in May and harvested in October (Chiang
386 et al., 2014). Hence, the higher nutrient levels were likely associated with the removal of fertilizers from the soil during
387 spring and summer.

388 **4.2 Equivalent impacts of CP- and EP-El Niño on water quality in specific watersheds**

389 Section 3 discussed the impacts of El Niño on water quality at the outlets and sub-basin scales. At the outlets, EP-El Niño
390 had a much greater impact on TN and TP than CP-El Niño both at annual and seasonal time scales. But at the sub-basin scale,
391 CP- and EP-El Niño could have equivalent impacts on water quality in specific watersheds, predominantly in Iowa (IA),
392 Illinois (IL), Minnesota (MN), Wisconsin (WI), and Indiana (IN), which contributed the greatest amounts of nutrient change
393 to the whole basin loads (Fig. 3). Table 4 listed the top 10 HUC-8 sub-basins with the largest nutrient change during the two
394 types of El Niño years. In EP-ENYs, TN anomalies changed from 6.2 and 11.7 kg ha⁻¹ among the top 10 HUC-8 sub-basins;
395 while in CP-ENYs, TN anomalies changed from 5.6 and 9.3 kg ha⁻¹ (Table 4). These changes in TN during classic El Niño
396 and El Niño Modoki were comparable. Analysis of the top 10 HUC-8 sub-basins with the largest TP change during the EP-
397 and CP-El Niño illustrated similar results (not shown). These findings indicated that CP-El Niño could have comparable
398 impacts on TN and TP as EP-El Niño at the hot spot sub-basins although EP-El Niño had a much broader and longer impact
399 on water quality at the outlets.

400
401
402
403
404
405
406
407
408
409
410

411 **Table 4.** Information on the top 10 8-digit Hydrologic Unit Codes (HUC-8) sub-basins with greatest TN anomalies during
 412 EP- and CP-El Niño years.

El Niño Type	HUC-8	TN (kg ha ⁻¹)		Precipitation (mm yr ⁻¹)		Cropland Percentage (%)	States
		Average	Anomaly	Average	Anomaly		
EP	07080102	51.2	-11.7	912.9	-54.8	70.1	IA,MN
	07080201	33.7	-10.8	909.9	-51.1	73.5	IA,MN
	07090006	37.8	-10.4	935.2	-65.7	68.8	IL,WI
	07020011	28.3	-8.5	845.1	-84.0	78.6	MN
	07080202	27.4	-7.5	890.2	-32.9	72.1	IA,MN
	05120107	24.8	-7.2	1068.8	-102.2	73.8	IN
	07090007	31.2	-6.9	949.4	-87.6	78.9	IL
	07080204	33.0	-6.6	918.0	-69.4	76.0	IA
	07080208	27.0	-6.3	904.4	-62.1	59.9	IA
	07080209	25.6	-6.2	914.8	-94.9	58.4	IA
CP	07080103	26.2	9.3	948.0	142	70.2	IA
	07080208	27.0	9.1	904.4	135	59.9	IA
	07080206	21.9	9.1	923.1	128	63.3	IA
	07090007	31.2	7.3	949.4	62	78.9	IL
	07080203	24.2	6.8	855.4	124	68.1	IA,MN
	07080102	51.2	6.5	912.9	51	70.1	IA,MN
	07020007	16.5	6.1	778.0	69	73.2	MN
	07090006	37.8	5.9	935.2	18	68.8	IL,WI
	07060006	24.4	5.6	911.8	44	59.3	IA
	07130009	20.6	5.6	1005.0	124	80.9	IL

413 **4.3 Biogeochemical process variation due to temperature change**

414 The effect of temperature on water quality through affecting evaporation and runoff has been analyzed in Section 3.2.2. In
 415 fact, the temperature can also affect water quality through some biochemical processes of nutrients (Neitsch et al., 2011). In
 416 order to analyze the biogeochemical process variations due to temperature changes during EP- and CP-El Niños, new
 417 analyses on nitrogen and phosphorus components, such as nitrate, organic nitrogen, soluble phosphorus, mineral phosphorus,
 418 and organic phosphorus had been carried out. Results from the analyses demonstrated that compared to precipitation,
 419 temperature plays a secondary role in altering nutrient levels through biogeochemical processes. Taking nitrate as an
 420 example, we showed the composite results of annual and seasonal nitrate anomalies (Figs. S6 and S7), respectively, during
 421 EP- and CP-El Niños. Figures S6 and S7 indicated that the pattern of nitrate was more similar to that of precipitation (Figs.
 422 6a, 6c, and 7a-7h) but different from that of temperature (Figs. 8a, 8c, and 9a-9h) in the Corn Belt region during El Niños.

423 This could be further confirmed by the pattern correlation results. The correlation coefficients of annual nitrate and
424 precipitation were 0.47, 0.36, 0.22, and 0.39, respectively, at OTRB and UMRB during EP- and CP-El Niños. The
425 correlation coefficients between nitrate and temperature were relatively small (the coefficients were -0.15, 0.08, 0.30, and -
426 0.31, respectively). The coefficient values altered between positive and negative at the two basins during EP- and CP-El
427 Niños. The inconsistent relationships between nitrate and temperature were mainly because the nitrate content could vary
428 through nitrification, mineralization, denitrification, and plant uptake processes (Neitsch et al., 2011). When the temperature
429 rises, the former two processes increase nitrate content, but the latter two decrease nitrate content. Thus, the final sign of the
430 correlation coefficient between nitrate and temperature really depends on the dominant processes. Similar results were also
431 found at seasonal scales (not shown). These results indicated that nitrate variations were dominated by precipitation
432 variations in the two basins during EP- and CP-El Niños, instead of temperature impacts on the biogeochemical processes.
433 Similar results were also found for other nutrient components, such as organic nitrogen, soluble phosphorus, mineral
434 phosphorus, and organic phosphorus (not shown).

435 **4.4 Future water quality change**

436 Existing studies suggested that CP-El Niño episodes occurred more frequently in a warming climate (Yeh et al., 2009; Yu et
437 al., 2010). We found that annual loads of TN and TP tend to increase in the Corn Belt region during CP-ENYs in the current
438 climate. As CP-El Niño frequency increases in the future, TN and TP loads would likely increase over the Corn Belt region
439 even under the same agricultural conditions, indicating a possible deterioration of water quality in this region when the
440 climate warms.

441 The spatial patterns of TN and TP anomalies during CP-ENYs (Fig. S8) also suggested that specific watersheds,
442 predominantly in southern UMRB and western OTRB, such as Iowa, Illinois, Wisconsin, Indiana, and Kentucky, will likely
443 experience the most increases of TN and TP loads in the future. Such information is critical to ensure proper decision-
444 making for watershed protection.

445 **4.5 Limitations and future work**

446 The model evaluation suggested that SWAT reasonably captured the hydrological and water quality behaviors in the Corn
447 Belt. However, this result could be influenced by the uncertainty of model simulations. For example, the limited number of
448 observation sites might bring uncertainties on the regional scales. The model was assessed by the best available observation
449 data, and the good agreement between the calculations and observations at 15 sites showed that the model reasonably
450 captured the changes in the water flow, TN, and TP. However, further assessment of the model is needed when more
451 observations are available.

452 The impacts of irrigation on runoff and nutrient levels were not analyzed in the study due to a lack of irrigation data over
453 the Corn Belt. Existing documents suggest that vast acreages of corn and soybeans are watered by center pivot irrigation in
454 the region, which uses an apparatus that sprays water across a field with a 75–90% efficiency, thus irrigation water mostly

455 infiltrates into the soil (Grassini et al., 2011; 2014; Green et al., 2018). In other words, precipitation likely plays a dominant
456 role in runoff; we thus focus on the impact of precipitation on runoff and water quality in the study. Further discussions on
457 irrigation are needed once detailed irrigation data are available.

458 In addition, as Chen et al. (2021) suggested that the CP-El Niño needed to be further classified into CP-I and CP-II types
459 due to the differences in sea surface temperature (SST) evolution patterns and climate impacts, the distribution of nutrients in
460 these two CP-El Niños might also differ and therefore are needed to be further studied in the future.

461 **5 Conclusions**

462 The impacts of EP- and CP-El Niños on water quality were investigated by using the SWAT model in the U.S. Corn Belt
463 region. Calibration and validation results indicated that the simulated streamflow and water quality generally agreed with
464 observations at most USGS gages. Then, the common features of the annual and seasonal loads of TN and TP for the EP-
465 and CP-El Niño events in the OTRB and UMRB were analyzed using a composite method based on the simulation results
466 during 1975–2016.

467 Annual composite results suggested that TN and TP loads decreased by 13.1% and 14.0% during EP-ENYs, respectively,
468 whereas they increased by 3.3% and 4.6% during CP-ENYs at the outlet of the OTRB, respectively. TN and TP also showed
469 a similar pattern at the outlet of the UMRB (18.5% and 19.8% reductions during EP-ENYs, and 5.7% and 4.4% increases
470 during CP-ENYs, respectively). Furthermore, more sub-basins showed negative annual anomalies of TN and TP during EP-
471 ENYs with maximum reductions up to -11.7 and -0.9 kg ha⁻¹, which were comparable to the normal year mean values (12.7
472 kg of N ha⁻¹ and 1.0 kg of P ha⁻¹), respectively, whereas they showed positive anomalies during CP-ENYs.

473 Seasonal composite results confirmed that water quality anomalies showed opposite patterns during EP-ENYs and CP-
474 ENYs and the changes in the water quality matched the ENSO phases at the outlet of the OTRB. Maximum reduction or
475 increase of the nutrients during EP-ENYs or CP-ENYs, respectively, occurred in winter, the peak season of El Niño. At the
476 outlet of the UMRB (corn-growing region), TN and TP anomalies were also influenced by agriculture activities and became
477 greater in spring and summer during both EP-ENYs and CP-ENYs, in consistent with the distribution of rainfall changes in
478 the basin. These results suggested that small changes in climate variables such as precipitation in the growing season could
479 have greater impacts on water quality in the UMRB during El Niño events.

480 Our analysis also found that at the outlets of UMRB and OTRB, EP-El Niño had a much greater impact on TN and TP
481 than CP-El Niño at both annual and seasonal time scales; but CP-El Niño could have comparable impacts on water quality as
482 EP-El Niño at specific watersheds or hot spots, predominantly in Iowa, Illinois, Minnesota, Wisconsin, and Indiana, which
483 contributed the greatest amounts of nutrient change to the whole basin loads.

484 Examination of the climate factors/processes on water quality change indicated that El Niño-induced precipitation and
485 temperature changes altered runoff and evaporation, and thus TN and TP in both UMRB and OTRB on annual and seasonal
486 time scales, as well as at the outlet and sub-basin scales. It is also found that nutrient levels were largely determined by

487 precipitation through runoff during both EP- and CP-ENYs, especially at the outlet, as the precipitation was a major source
488 of runoff, and nitrogen and phosphorus components were transported by runoff. At the sub-basin scale, water quality was
489 affected by the combination of precipitation and agricultural activities, especially in the UMRB during the growing season.

490 In the future when the climate continues to warm, the CP-El Niño episode is projected to occur more frequently, TN and
491 TP loads might increase in the Corn Belt region even under the same agricultural conditions, while water quality would
492 generally get better in EP-El Niño years. The findings from this study may help ensure proper decision-making for
493 watershed protection and possible ways to address anticipated water quality change associated with El Niño events.

494

495 **Data availability.** Available upon request.

496 **Author Contributions.** W.L. and P.C. designed the research; P.C. and K.H. performed the data collection and model
497 calculation; W.L. and P.C. contributed to the interpretation of the results; P.C. and W.L. wrote the manuscript.

498 **Competing Interests.** The authors declare no competing interests.

499 **Disclaimer.** Publisher's note: Copernicus Publications remains neutral with regard to jurisdictional claims in published maps
500 and institutional affiliations.

501 **Acknowledgments.** We thank Dr. Yongping Yuan for the suggestions on simulations of water quality in the OTRB and
502 UMRB. This research was supported by the Shanxi Province Science Foundation for Youths, China (No. 202103021223106,
503 202103021223079 and 20210302124458), the Research Project Supported by Shanxi Scholarship Council of China (No.
504 2022-080 and 2021-051), the Shanxi Province Water Science and Technology Research and Promotion Project, China (No.
505 2022GM023 and 2022GM017) the National Key Research and Development Program, China (No. 2018YFC0406406), the
506 China Scholarship Council (File No. 201806935023), the Institute-Local Cooperation Project of the Chinese Academy of
507 Engineering (No. 2020SX8), the Government Financial Grants Project, China (No. ZNGZ2015-036), the Key Research and
508 Development Program (Social Development Field) of Shanxi Province, China (No. 201903D321052), and the Natural
509 Science Foundation of Shanxi Province, China (No. 201901D111059 and 201901D111060).

510

511 **References**

512 Abbaspour, H., Saeidi-Sar, S., Afshari, H. and Abdel-Wahhab, M. A.: Tolerance of Mycorrhiza infected Pistachio (*Pistacia*
513 *vera* L.) seedling to drought stress under glasshouse conditions, *J. Plant Physiol.*, 169(7), 704–709,
514 doi:10.1016/j.jplph.2012.01.014, 2012.

515 Afonso de Oliveira Serrão, E., Silva, M. T., Ferreira, T. R., Paiva de Ataíde, L. C., Assis dos Santos, C., Meiguins de Lima,
516 A. M., de Paulo Rodrigues da Silva, V., de Assis Salviano de Sousa, F. and Cardoso Gomes, D. J.: Impacts of land use
517 and land cover changes on hydrological processes and sediment yield determined using the SWAT model, *Int. J.*
518 *Sediment Res.*, doi:10.1016/j.ijsrc.2021.04.002, 2022.

519 Arnold, J. G., Srinivasan, R., Muttiah, R. S. and Williams, J. R.: Large area hydrologic modeling and assessment part I:
520 Model development, *J. Am. Water Resour. Assoc.*, 34(1), 73–89, doi:10.1111/j.1752-1688.1998.tb05961.x, 1998.

521 Baker, N. T.: Tillage practices in the conterminous United States, 1989–2004 — Datasets aggregated by watershed, *Data*
522 *Series 573*: <http://pubs.usgs.gov/ds/ds573/pdf/dataseries573final.pdf>, 2011.

523 Bales, R. C., Goulden, M. L., Hunsaker, C. T., Conklin, M. H., Hartsough, P. C., O’Geen, A. T., Hopmans, J. W., and Safeeq,
524 M.: Mechanisms controlling the impact of multi-year drought on mountain hydrology, *Sci. Rep.*, 8, 690,
525 <https://doi.org/10.1038/s41598-017-19007-0>, 2018.

526 Chaplot, V., Saleh, A., Jaynes, D. B. and Arnold, J.: Predicting water, sediment and NO₃-N loads under scenarios of land-use
527 and management practices in a flat watershed, *Water. Air. Soil Pollut.*, 154(1–4), 271–293,
528 doi:10.1023/B:WATE.0000022973.60928.30, 2004.

529 Chen, M., Chang, T. H., Lee, C. T., Fang, S. W. and Yu, J. Y.: A study of climate model responses of the western Pacific
530 subtropical high to El Niño diversity, *Clim. Dyn.*, 56(1–2), 581–595, doi:10.1007/s00382-020-05500-2, 2021.

531 Chen, P., Yuan, Y., Li, W., LeDuc, S. D., Lark, T. J., Zhang, X. and Clark, C.: Assessing the Impacts of Recent Crop
532 Expansion on Water Quality in the Missouri River Basin Using the Soil and Water Assessment Tool, *J. Adv. Model.*
533 *Earth Syst.*, 13(6), doi:10.1029/2020MS002284, 2021.

534 Chiang, L. C., Yuan, Y., Mehaffey, M., Jackson, M., and Chaubey, I.: Assessing SWAT’s performance in the Kaskaskia
535 River watershed as influenced by the number of calibration stations used, 28, 676–687,
536 <https://doi.org/10.1002/hyp.9589>, 2014.

537 Gassman, P. W., Reyes, M. R., Green, C. H. and Arnold, J. G.: The soil and water assessment tool: Historical development,
538 applications, and future research directions, *Trans. ASABE*, 50(4), 1211–1250, 2007.

539 Gershunov, A.: ENSO influence on intraseasonal extreme rainfall and temperature frequencies in the contiguous United
540 States: Implications for long-range predictability, *J. Clim.*, 11(12), 3192–3203, doi:10.1175/1520-
541 0442(1998)011<3192:EIOIER>2.0.CO;2, 1998.

542 Grassini, P., Yang, H., Irmak, S., Thorburn, J., Burr, C., and Cassman, K. G.: High-yield irrigated maize in the Western U.S.
543 Corn Belt: II. Irrigation management and crop water productivity, *F. Crop. Res.*, 120, 133–141,
544 <https://doi.org/10.1016/j.fcr.2010.09.013>, 2011.

545 Grassini, P., Torrión, J. A., Cassman, K. G., Yang, H. S., and Specht, J. E.: Drivers of spatial and temporal variation in
546 soybean yield and irrigation requirements in the western US Corn Belt, 163, 32–46,
547 <https://doi.org/10.1016/j.fcr.2014.04.005>, 2014.

548 Green, T. R., Kipka, H., David, O., and McMaster, G. S.: Where is the USA Corn Belt, and how is it changing?, *Sci. Total*
549 *Environ.*, 618, 1613–1618, <https://doi.org/10.1016/j.scitotenv.2017.09.325>, 2018.

550 Johnson, M. V. V., Norfleet, M. L., Atwood, J. D., Behrman, K. D., Kiniry, J. R., Arnold, J. G., White, M. J. and Williams,
551 J.: The Conservation Effects Assessment Project (CEAP): A national scale natural resources and conservation needs
552 assessment and decision support tool, in *IOP Conference Series: Earth and Environmental Science*, vol. 25., 2015.

553 Kao, H. Y. and Yu, J. Y.: Contrasting Eastern-Pacific and Central-Pacific types of ENSO, *J. Clim.*, 22(3), 615–632,
554 doi:10.1175/2008JCLI2309.1, 2009.

555 Keener, V. W., Feyereisen, G. W., Lall, U., Jones, J. W., Bosch, D. D. and Lowrance, R.: El-Niño/Southern Oscillation
556 (ENSO) influences on monthly NO₃ load and concentration, stream flow and precipitation in the Little River
557 Watershed, Tifton, Georgia (GA), *J. Hydrol.*, 381(3–4), 352–363, doi:10.1016/j.jhydrol.2009.12.008, 2010.

558 Kellner, O. and Niyogi, D.: Climate variability and the U.S. corn belt: Enso and AO episode-dependent hydroclimatic
559 feedbacks to corn production at regional and local scales, *Earth Interact.*, 19(6), 1–32, doi:10.1175/EI-D-14-0031.1,
560 2015.

561 Kumar, K. K., Rajagopalan, B., Hoerling, M., Bates, G. and Cane, M.: Unraveling the mystery of Indian monsoon failure
562 during El Niño, *Science* (80-), 314(5796), 115–119, doi:10.1126/science.1131152, 2006.

563 Laken, B. A. and Čalogović, J.: Composite analysis with monte carlo methods: An example with cosmic rays and clouds, 3,
564 <https://doi.org/10.1051/swsc/2013051>, 2013.

565 Larkin, N. K. and Harrison, D. E.: On the definition of El Niño and associated seasonal average U.S. weather anomalies,
566 *Geophys. Res. Lett.*, 32(13), 1–4, doi:10.1029/2005GL022738, 2005.

567 Lee, S. K., Mapes, B. E., Wang, C., Enfield, D. B. and Weaver, S. J.: Springtime ENSO phase evolution and its relation to
568 rainfall in the continental U.S., *Geophys. Res. Lett.*, 41(5), 1673–1680, doi:10.1002/2013GL059137, 2014.

569 Li, W., Zhang, P., Ye, J., Li, L. and Baker, P. A.: Impact of two different types of El Niño events on the Amazon climate and
570 ecosystem productivity, *J. Plant Ecol.*, 4(1–2), 91–99, doi:10.1093/jpe/rtq039, 2011.

571 Mississippi River/Gulf of Mexico Watershed Nutrient Task Force: Gulf Hypoxia: Action Plan 2008 for Reducing, Mitigating
572 and Controlling Hypoxia in the Northern Gulf of Mexico and Improving Water Quality in the Mississippi River Basin,
573 in *Hypoxia in the Northern Gulf of Mexico*, pp. 265–305., 2011.

574 Mo, K. C.: Interdecadal modulation of the impact of ENSO on precipitation and temperature over the United States, *J. Clim.*,
575 23(13), 3639–3656, doi:10.1175/2010JCLI3553.1, 2010.

576 Moriasi, D. N., Gitau, M. W., Pai, N. and Daggupati, P.: Hydrologic and water quality models: Performance measures and
577 evaluation criteria, *Trans. ASABE*, 58(6), 1763–1785, doi:10.13031/trans.58.10715, 2015.

578 Neitsch, S. L., Arnold, J. G., Kiniry, J. R. and Williams, J. R.: Soil and Water Assessment Tool Theoretical Documentation
579 Version 2009, Available online: <http://hdl.handle.net/1969.1/128050>., 2011.

580 Pagliero, L., Bouraoui, F., Willems, P. and Diels, J.: Large-Scale Hydrological Simulations Using the Soil Water Assessment
581 Tool, Protocol Development, and Application in the Danube Basin, *J. Environ. Qual.*, 43(1), 145–154,
582 doi:10.2134/jeq2011.0359, 2014.

583 Panagopoulos, Y., Gassman, P. W., Arritt, R. W., Herzmann, D. E., Campbell, T. D., Jha, M. K., Kling, C. L., Srinivasan, R.,
584 White, M. and Arnold, J. G.: Surface water quality and cropping systems sustainability under a changing climate in the
585 Upper Mississippi River Basin, *J. Soil Water Conserv.*, 69(6), 483–494, doi:10.2489/jswc.69.6.483, 2014.

586 Panagopoulos, Y., Gassman, P. W., Jha, M. K., Kling, C. L., Campbell, T., Srinivasan, R., White, M. and Arnold, J. G.: A
587 refined regional modeling approach for the Corn Belt - Experiences and recommendations for large-scale integrated
588 modeling, *J. Hydrol.*, 524, 348–366, doi:10.1016/j.jhydrol.2015.02.039, 2015.

589 Panagopoulos, Y., Gassman, P. W., Kling, C. L., Cibin, R. and Chaubey, I.: Water Quality Assessment of Large-scale
590 Bioenergy Cropping Scenarios for the Upper Mississippi and Ohio-Tennessee River Basins, *J. Am. Water Resour.*
591 *Assoc.*, 53(6), 1355–1367, doi:10.1111/1752-1688.12594, 2017.

592 Paul, J. H., Rose, J. B., Jiang, S. C., Zhou, X., Cochran, P., Kellogg, C., Kang, J. B., Griffin, D., Farrah, S. and Lukasik, J.:
593 Evidence for groundwater and surface marine water contamination by waste disposal wells in the Florida Keys, *Water*
594 *Res.*, 31(6), 1448–1454, doi:10.1016/S0043-1354(96)00374-0, 1997.

595 Rabalais, N. N., Turner, R. E., Sen Gupta, B. K., Boesch, D. F., Chapman, P. and Murrell, M. C.: Hypoxia in the northern
596 Gulf of Mexico: Does the science support the plan to reduce, mitigate, and control hypoxia?, *Estuaries and Coasts*,
597 30(5), 753–772, doi:10.1007/BF02841332, 2007.

598 Ren, H. L., Lu, B., Wan, J., Tian, B., and Zhang, P.: Identification Standard for ENSO Events and Its Application to Climate
599 Monitoring and Prediction in China, *J. Meteorol. Res.*, 32, 923–936, <https://doi.org/10.1007/s13351-018-8078-6>, 2018.

600 Sanchez, S. C. and Karnauskas, K. B.: Diversity in the Persistence of El Niño Events Over the Last Millennium, *Geophys.*
601 *Res. Lett.*, 48, e2021GL093698, <https://doi.org/10.1029/2021GL093698>, 2021.

602 Santhi, C., Srinivasan, R., Arnold, J. G. and Williams, J. R.: A modeling approach to evaluate the impacts of water quality
603 management plans implemented in a watershed in Texas, *Environ. Model. Softw.*, 21(8), 1141–1157,
604 doi:10.1016/j.envsoft.2005.05.013, 2006.

605 Santhi, C., Kannan, N., White, M., Di Luzio, M., Arnold, J. G., Wang, X. and Williams, J. R.: An Integrated Modeling
606 Approach for Estimating the Water Quality Benefits of Conservation Practices at the River Basin Scale, *J. Environ.*
607 *Qual.*, 43(1), 177–198, doi:10.2134/jeq2011.0460, 2014.

608 Schwarz, G. E., Hoos, A. B., Alexander, R. B., and Smith, R. A.: The SPARROW Surface Water-Quality Model, *U.S. Geol.*
609 *Surv. Tech. Methods. Sect. B*, B. 6, 6-B3, 1–29, <https://water.usgs.gov/nawqa/sparrow/sparrow-mod.html>, 2006.

610 Sharma, S., Srivastava, P., Fang, X. and Kalin, L.: Incorporating climate variability for point-source discharge permitting in
611 a complex river system, *Trans. ASABE*, 55(6), 2213–2228, doi:10.13031/2013.42507, 2012.

612 Sun, G., Alstad, K., Chen, J., Chen, S., Ford, C. R., Lin, G., Liu, C., Lu, N., Menulty, S. G., Miao, H., Noormets, A., Vose, J.
613 M., Wilske, B., Zeppel, M., Zhang, Y., and Zhang, Z.: A general predictive model for estimating monthly ecosystem
614 evapotranspiration, 4, 245–255, <https://doi.org/10.1002/eco.194>, 2011.

615 Tan, W., Wei, Z., Liu, Q., Fu, Q., Chen, M., Li, B. and Li, J.: Different influences of two El Niño types on low-level
616 atmospheric circulation over the subtropical western North Pacific, *J. Clim.*, 33(3), 825–846, doi:10.1175/JCLI-D-19-
617 0223.1, 2020.

618 Tang, T., Li, W. and Sun, G.: Impact of two different types of El Niño events on runoff over the conterminous United States,
619 *Hydrol. Earth Syst. Sci.*, 20(1), 27–37, doi:10.5194/hess-20-27-2016, 2016.

620 Thaler, E. A., Larsen, I. J., and Yu, Q.: The extent of soil loss across the US Corn Belt, 118, 1–8,
621 <https://doi.org/10.1073/pnas.1922375118>, 2021.

622 Thomson, A. M., Brown, R. A., Rosenberg, N. J., Izaurralde, R. C., Legler, D. M. and Srinivasan, R.: Simulated impacts of
623 El Niño/Southern Oscillation on United States water resources, *J. Am. Water Resour. Assoc.*, 39(1), 137–148,
624 doi:10.1111/j.1752-1688.2003.tb01567.x, 2003.

625 Ting, M., Seager, R., Li, C., Liu, H. and Henderson, N.: Future Summer Drying in the U.S. Corn Belt and the Role of
626 Midlatitude Storm Tracks, *J. Clim.*, 34(22), 9043–9056, doi:10.1175/JCLI-D-20-1004.1, 2021.

627 Trenberth, K. E.: The Definition of El Niño, *Bull. Am. Meteorol. Soc.*, 78(12), 2771–2777, doi:10.1175/1520-
628 0477(1997)078<2771:TDOENO>2.0.CO;2, 1997.

629 Twine, T. E., Kucharik, C. J. and Foley, J. A.: Effects of El Niño-Southern Oscillation on the climate, water balance, and
630 streamflow of the Mississippi River basin, *J. Clim.*, 18(22), 4840–4861, doi:10.1175/JCLI3566.1, 2005.

631 USDA-NASS. (2016). CDL Online Website: <https://nassgeodata.gmu.edu/CropScape/>.

632 USDA-NASS. (2017). Census of Agriculture Online Website: <https://www.nass.usda.gov/AgCensus/>.

633 Vaché, K. B., Eilers, J. M. and Santelmann, M. V.: Water quality modeling of alternative agricultural scenarios in the U.S.
634 Corn Belt, *J. Am. Water Resour. Assoc.*, 38(3), 773–787, doi:10.1111/j.1752-1688.2002.tb00996.x, 2002.

635 Wang, H. and Asefa, T.: Impact of different types of ENSO conditions on seasonal precipitation and streamflow in the
636 southeastern United States, *Int. J. Climatol.*, 38(3), 1438–1451, doi:10.1002/joc.5257, 2018.

637 Wang, H. and Kumar, A.: Assessing the impact of ENSO on drought in the U.S. Southwest with NCEP climate model
638 simulations, *J. Hydrol.*, 526, 30–41, <https://doi.org/10.1016/j.jhydrol.2014.12.012>, 2015.

639 Wilks, D. S.: *Statistical Methods in the Atmospheric Sciences: An Introduction*. Academic press, 1995.

640 Williams, J. R., Arnold, J. G., Kiniry, J. R., Gassman, P. W. and Green, C. H.: History of model development at Temple,
641 Texas, in *Hydrological Sciences Journal*, vol. 53, pp. 948–960., 2008.

642 Yeh, S. W., Kug, J. S., Dewitte, B., Kwon, M. H. and Kirtman, B. P.: El Niño in a changing climate, *Nature*, 461, 511–514
643 [online] Available from:
644 [http://www.nature.com/nature/journal/v461/n7263/abs/nature08316.html%5Cnpapers2://publication/uuid/A3596821-](http://www.nature.com/nature/journal/v461/n7263/abs/nature08316.html%5Cnpapers2://publication/uuid/A3596821-0F46-4399-A217-04ED198F5C91)
645 [0F46-4399-A217-04ED198F5C91](http://www.nature.com/nature/journal/v461/n7263/abs/nature08316.html%5Cnpapers2://publication/uuid/A3596821-0F46-4399-A217-04ED198F5C91), 2009.

646 Yen, H., Daggupati, P., White, M. J., Srinivasan, R., Gossel, A., Wells, D., and Arnold, J. G.: Application of large-scale,
647 multi-resolution watershed modeling framework using the Hydrologic and Water Quality System (HAWQS), 8,
648 <https://doi.org/10.3390/w8040164>, 2016.

649 Yu, J. Y., Kao, H. Y. and Lee, T.: Subtropics-related interannual sea surface temperature variability in the central equatorial
650 pacific, *J. Clim.*, 23(11), 2869–2884, doi:10.1175/2010JCLI3171.1, 2010.

651 Zhang, H., Wang, B., Liu, D. L., Zhang, M., Leslie, L. M. and Yu, Q.: Using an improved SWAT model to simulate
652 hydrological responses to land use change: A case study of a catchment in tropical Australia, *J. Hydrol.*,
653 doi:10.1016/j.jhydrol.2020.124822, 2020.